Beilstein-Institut

Cracking the Sugar Code by Navigating the Glycospace
June 27th – July 1st, 2011, Potsdam, Germany

Biophysical Studies on the Interactions of Bacterial Toxins

W. Bruce Turnbull

School of Chemistry and Astbury Centre for Structural Molecular Biology, University of Leeds, Leeds, LS2 9JT, U.K.

E-Mail: w.b.turnbull@leeds.ac.uk

Received: 12th January 2012 / Published: 11th July 2012

Abstract

Many diarrhoeal diseases such as cholera are caused by protein toxins that have an AB_5 hetero-oligomeric structure. The proteins comprise a single toxic A-subunit and a pentameric B-subunit that interacts with specific cell surface glycolipids. Inhibitors of such protein-carbohydrate interactions could provide prophylactic treatments for these debilitating diseases. In our work we aim to understand the binding interactions of multivalent inhibitors for bacterial toxins. Often a single biophysical technique is limited in the information it can provide, whereas a more complete picture can be constructed through an integrated approach using a broad range of biophysical methods. For example, the importance of protein and ligand dynamics in multivalent interactions is revealed when combinations of NMR spectroscopy, isothermal titration calorimetry, analytical ultracentrifugation and dynamic light scattering are used to study to different multivalent systems.

Introduction

A variety of enteropathogenic bacteria including *Vibrio cholerae* and some strains of *Escherichia coli* release protein toxins into the intestine of their host [1]. The toxins bind to specific glycolipid ligands on the surface of the cells that line the intestine. Following endocytosis and retrograde trafficking to the endoplasmic reticulum, the toxins are translocated into the cytosol where they initiate the biochemical events leading to potentially fatal

diarrhoea [2]. Many of these bacterial toxins share a common AB_5 architecture in which a single toxic A-subunit is non-covalently associated with a cyclic pentamer of B-subunits [1]. While the B-pentamer is not itself toxic, it constitutes the carbohydrate-binding domain of the toxin and is thus essential for entry into cells. Therefore, inhibitors of these protein-carbohydrate interactions have potential as anti-diarrhoeal drugs.

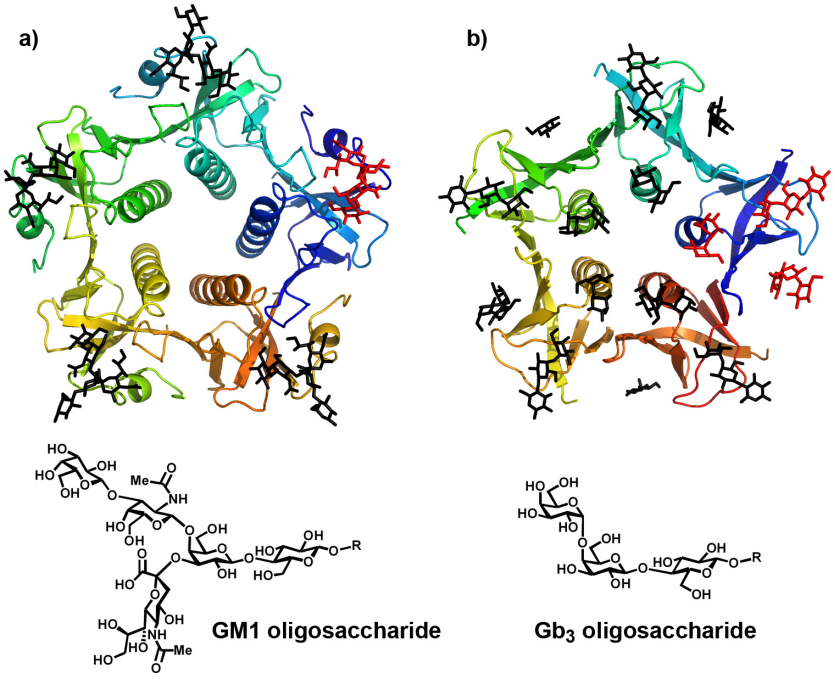

Figure 1. (a) Cholera toxin B-pentamer (CTB) and **(b)** verotoxin B-pentamer (VTB) with their carbohydrate ligands GM1 and Gb_3, respectively. The carbohydrate structures highlighted in red indicate how many oligosaccharides bind to each protomer. The structures were prepared in PyMOL using Protein Data Bank files 3CHB.pdb and 1BOS.pdb.

Cholera toxin and verotoxin (also known as shiga-like toxin 1) are the most widely studied examples of AB_5 bacterial toxins. Although the B-subunits of these two toxins have essentially no sequence similarity [1], they have evolved to have the same protein fold and to function as lectins for glycolipids (Figure 1). They differ in the number and structure of the carbohydrates that they recognise: cholera toxin B-pentamer (CTB) has one binding per subunit for the branched pentasaccharide of ganglioside GM1 [3], while the verotoxin B-pentamer (VTB) has three binding sites per subunit for the trisaccharide portion of globotriaosyl ceramide (Gb3) [4]. More significant, however, is the difference in affinity of these interactions. The CTB-GM1 interaction is one of the highest affinity protein-carbohydrate interactions known with a dissociation constant (K_d) of 40 nM [5], whereas the highest affinity of the three binding sites on VTB has only a 1 mM K_d [6]. However, as all 15 of the

binding sites on the VTB pentamer are arranged on the same face of the protein [4], it is possible for VTB to make many simultaneous interactions with Gb3 glycolipids in the cell membrane. Multivalent binding of this type is characteristic of most protein-carbohydrate interactions and can transform weak millimolar dissociation constants into sub-nanomolar avidities that are functionally useful [7 – 10]. In the case of VTB, it is clear that multivalency is absolutely essential for its function, but CTB also benefits from making multivalent interactions to enhance binding and facilitate the rate of endocytosis [11].

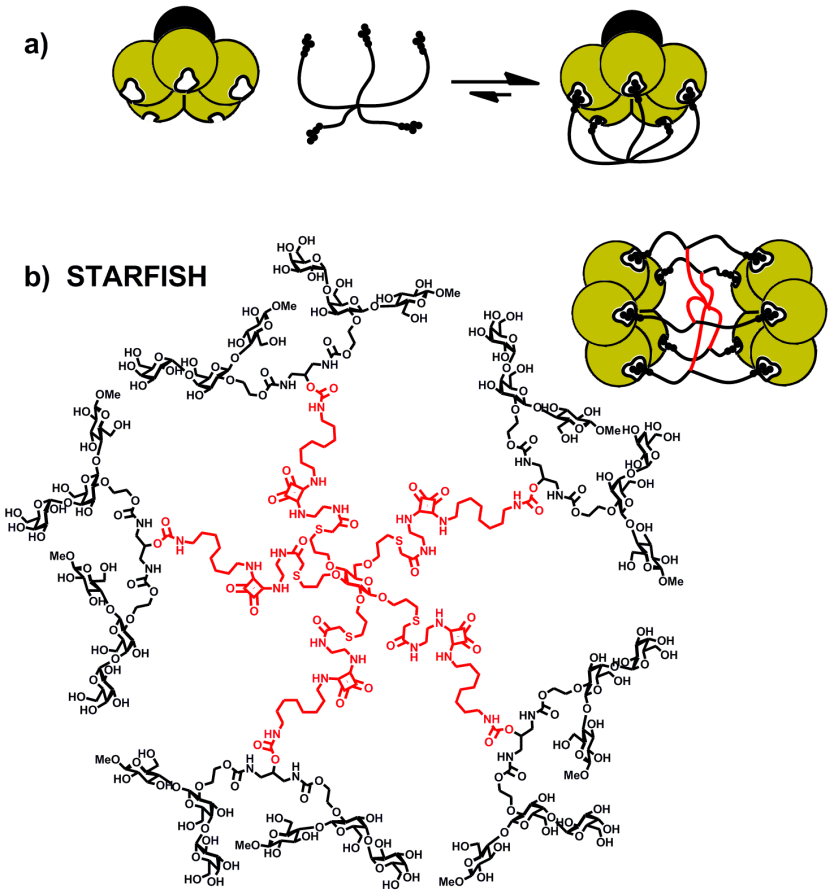

Figure 2. (a) cartoon representation of a pentavalent ligand binding to an AB_5 bacterial toxin; **(b)** Bundle's STARFISH ligand that can crosslink two VTB pentamers to form a sandwich complex.

Just as multivalency is important for biological function, it also provides a powerful strategy for inhibiting protein-carbohydrate interactions [7, 12]. If one could design a scaffold that could place a carbohydrate ligand into each protein binding site simultaneously (Figure 2a), then even if any individual oligosaccharide were to dissociate from the protein, the other

ligand groups would hold it in close proximity to the protein surface, thus increasing the effective concentration of the oligosaccharide, and thus the probability of its rebinding to the protein. Multivalent inhibition can operate by several mechanisms including: chelation of binding sites; statistical increases in effective concentration; and aggregation mechanisms [8]. Dissecting multivalent inhibition mechanisms is thus a challenging pursuit, but can be achieved by using a combination of complementary biophysical techniques as illustrated by the following two case studies.

Multivalent Binding Influenced by Protein Dynamics

One of the most celebrated examples of multivalent inhibition is Bundle's "STARFISH" ligand for VTB (Figure 2b) [13]. The molecule comprises a pentavalent core derived from a modified glucose residue with five flexible arms, each of which bares two copies of the Gb3 trisaccharide. STARFISH was over a million times more active as an inhibitor of VTB adhesion than the parent monovalent Gb3 trisaccharide, thus demonstrating the power of the multivalent inhibition strategy.

The ligand was designed to crosslink two of the Gb3 binding sites in each of the five VTB subunits. However, a crystal structure of the VTB-STARFISH complex revealed that the carbohydrate ligand groups occupied only the highest affinity of the three binding sites on each protomer [13]. The remaining five Gb3 ligand groups instead engaged a second VTB pentamer to make a ternary sandwich complex (Figure 2b). While this could be interpreted as an artefact of the crystallisation procedure, subsequent studies suggested that the dimer of pentamers also formed in solution [14]. Although the inhibitor was very potent, the structural studies raised doubts about whether the divalent Gb3 groups at the end of each of the STARFISH arms were capable of simultaneous binding to sites 1 and 2 on the VTB surface. However, an NMR shift-perturbation experiment using ^{15}N-enriched protein confirmed that a divalent Gb3 ligand (Figure 3c) could indeed interact with both sites 1 and 2 on VTB [15].

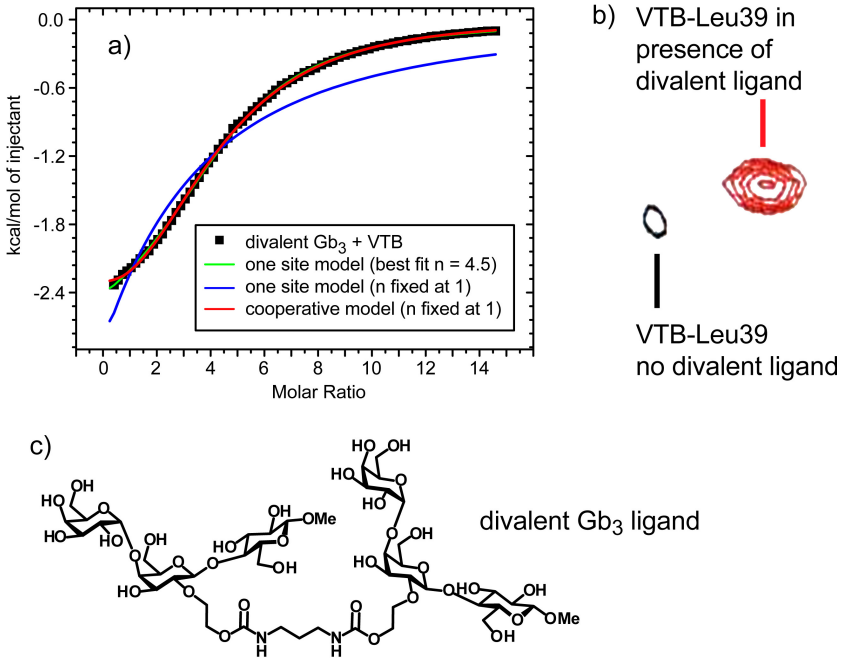

Figure 3. (a) ITC data for a titration of **(c)** divalent Gb3 ligand into a solution of VTB. The binding stoichiometry values (n) represent the number of divalent ligands binding to each protomer of VTB. **(b)** Signals from a ^{1}H-^{15}N HSQC NMR titration of divalent Gb_3 into a solution of ^{15}N-enriched VTB; the data show a significant increase in signal intensity for the Leu39 amide bond upon addition of the ligand.

Intrigued by the apparent differences in complexation for the divalent and decavalent ligands, we sought to measure the binding thermodynamics of the divalent ligand using isothermal titration calorimetry (ITC). This technique provides direct access to binding affinities, enthalpies and also to binding stoichiometries, in ideal cases. However, fitting the ITC data to a standard one-site model suggested that 4.5 divalent ligands bound to each VTB protomer (i. e., 22.5 divalent ligands per VTB pentamer) [16]. As such a high binding stoichiometry is not feasible in this system; the sigmoidal shape of the curve (Figure 3a) must be attributed to a different phenomenon.

Closer inspection of the shift-perturbation NMR data revealed that a number of the HSQC signals became more intense upon addition of the ligand (Figure 3) [16]. Such observations can be indicative of changes in protein dynamics upon binding. If a protein can interconvert between two different conformations, the observed NMR signal will be dependent on the rate of the interconversion process. In the fast exchange regime, the conformers interconvert many times during the timescale of the NMR experiment, giving rise to a single sharp signal in the NMR spectrum which represents the average of the different states. Conversely, when the interconversion process is slow, two separate signals will be observed; however, they

will be weighted according to the population of the species present, and so may also give rise to essentially a single sharp signal in cases where one conformer is dominant. At intermediate exchange rates, the signals become broadened and thus lower in intensity. We considered it likely that the sharpening of the signals in the NMR titration data corresponded to a shift from intermediate to slow exchange upon binding the ligand. A relaxation dispersion experiment was used to confirm that the changes in line shape were associated with a chemical exchange process that disappeared upon addition of the ligand [16]. Furthermore, the exchange phenomenon was most pronounced for residues at the interface between the protomer subunits.

So what is the nature of the chemical exchange phenomenon? Most X-ray and NMR spectroscopy structures of VTB show the pentamer to have a symmetrical doughnut shape [4, 17]; however, the original crystal structure of the protein displayed a helical shape, reminiscent of a lock washer, in which two adjacent protomers were displaced by two amino acid residues along a β-sheet interface (Figure 4) [18]. Interconversion of the lock washer and symmetrical conformers of the protein would likely give rise to exchange broadening in the initial NMR spectra, but if the divalent ligand bound selectively to only the symmetric conformer, then the exchange process would be lost upon formation of the complex.

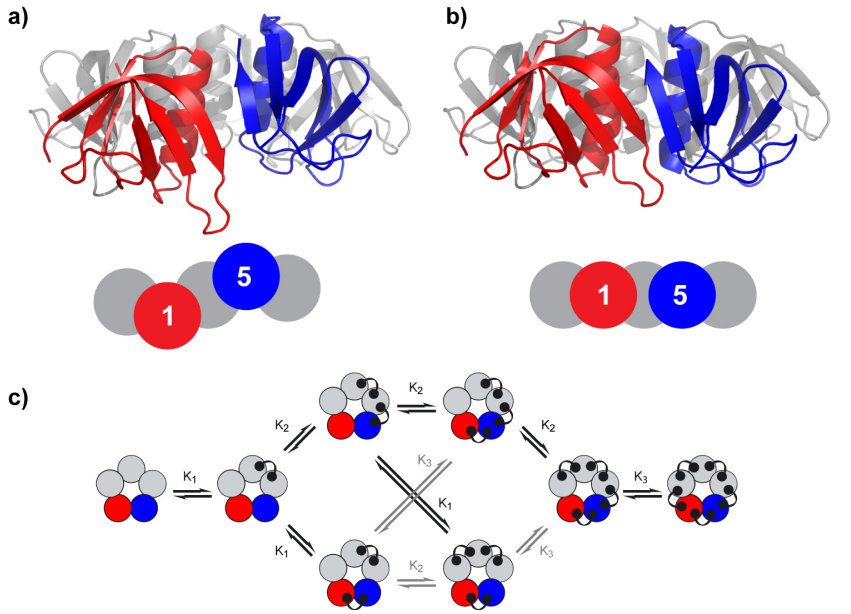

Figure 4. (a) "Lockwasher" and **(b)** "doughnut" conformations of VTB (from Protein databank files 1BOV.pdb and 1BOS.pdb, respectively). **(c)** Binding model for a divalent ligand binding to a pentavalent protein: K_1 is for binding to an isolated site, K_2 for binding to a site that is already occupied and K_3 for binding between two occupied sites; however, K_1 followed by K_3 is equivalent to K_2 followed by K_2 and so only two association constants are required to describe the system.

This hypothesis has thermodynamic consequences as loss of protein dynamics will incur an entropic penalty. However, as the pentamer will become increasingly rigid as the VTB binding sites fill up, then the system will pay a lower entropic penalty when the final ligand binds than it did for the first ligand. In other words, the system should display positive cooperativity. In order to test the hypothesis, we implemented a more sophisticated model for fitting the ITC data, in which all possible complexes (1:1, 1:2, 1:3, etc.) were considered explicitly (Figure 4) [16]. By making an assumption that any cooperative effects would only arise though interactions between nearest neighbour protomer subunits, it was possible to simplify the model to two stepwise *association* constants with corresponding enthalpy changes. K_1 represents the first ligand to bind to a pentamer, while K_2 corresponds to the average stepwise association constant once all binding sites have been filled. The ITC fitting results confirmed that the system displayed weak positive cooperativity and that the entropy change became more favourable (actually less unfavourable) as the titration proceeded (Table 1). However, the improvement in the entropic term was largely offset by a substantial decrease in the favourable enthalpy term as the pentamer became rigidified. This observation indicates that flexibility in the pentamer is entropically favourable, but the symmetric conformer is enthalpically favoured.

Table 1. Thermodynamic parameters for divalent Gb3 binding to VTB using the model outlined in Figure 4.

$K_1 = 114 \pm 2.2\ M^{-1}$	$K_2 = 283 \pm 4.5\ M^{-1}$
$\Delta H_1^\circ = -27.8 \pm 0.13$ kJ/mol	$\Delta H_2^\circ = -12.0 \pm 0.02$ kJ/mol
$T\Delta S_1^\circ = -24.8 \pm 0.13$ kJ/mol	$T\Delta S_1^\circ = -8.4 \pm 0.02$ kJ/mol

In summary, NMR spectroscopy indicated that the divalent ligand could bind to the protein as originally designed; however, it was only with a combination of NMR, X-ray crystallography and ITC that the importance and mechanism of protein dynamics for attenuating the divalent binding was revealed.

Multivalent Binding Influenced by Ligand Dynamics

Similar pentameric and decameric inhibitors have been reported by Fan and Hol [19, 20] for the B-pentamers of cholera toxin (CTB) and the closely related *E. coli* heat-labile toxin (LTB) which is 80% identical to CTB [1]. While these valency-matched inhibitors form the expected 1:1 and 1:2 complexes with their protein targets, we have found that a series of multivalent inhibitors with mismatched valencies prepared by Pieters, Visser and Zuilhof [21], inhibit CTB/LTB adhesion by aggregative mechanisms [22].

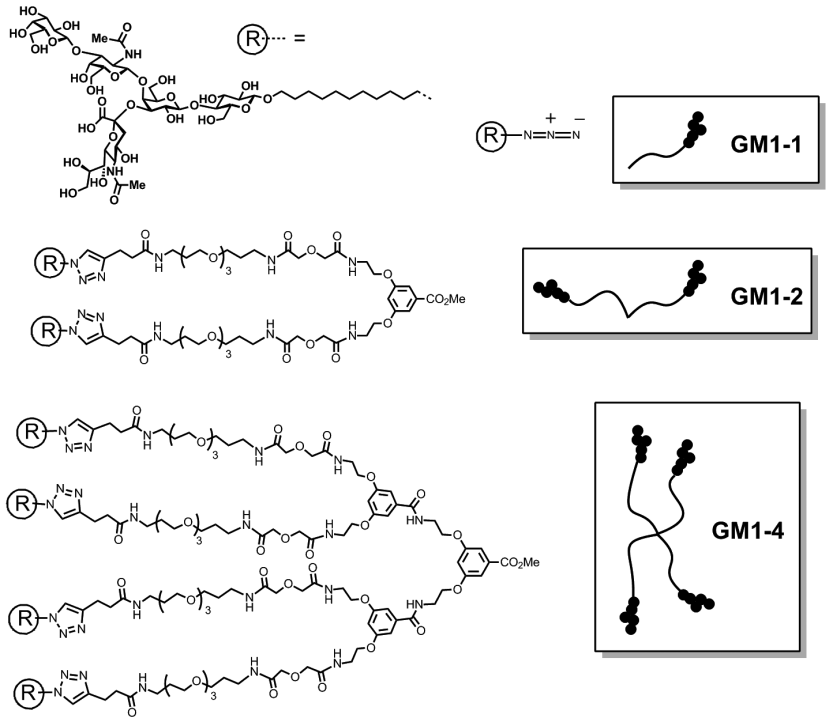

Figure 5. Chemical structures of monovalent and multivalent GM1-based inhibitors.

Compounds comprising two or four GM1 oligosaccharides attached to flexible scaffolds (**GM1 – 2** and **GM1 – 4**, respectively; (Figure 5) were found to be up to 20,000 times more potent as inhibitors of CTB or LTB adhesion than monovalent ligand **GM1 – 1** when compared in an ELISA assay [21, 22]. However, we found only marginal affinity enhancements when each ligand was studied by ITC. It was as if each GM1 group was behaving independently of one another in the ITC experiment, even though the divalent and tetravalent ligands were much more potent in the inhibition assay. Upon closer inspection of the solutions recovered from the ITC, it was noticed that the samples had become hazy during the titration. Therefore the mixtures were studied further by analytical ultracentrifugation (AUC) and dynamic light scattering (DLS), which are all techniques better suited for the study of aggregation phenomena.

In a sedimentation velocity AUC experiment, the protein solution is spun rapidly in a specialised centrifuge that has an optical system to record the UV-absorbance as a function of distance across the sample cell [23]. As the UV absorbance at 280 nm corresponds to the protein concentration, it is possible to follow the process of protein sedimentation in real time while the sample is spinning in the centrifuge. Application of the Svedberg and Lamm equations to the time-dependent data in the SEDFIT program provides a simple depiction of

the relative concentrations of different sized species present in the mixture [24]. The LTB pentamer gave rise to a single peak in the c(S) plot (Figure 6a) that corresponds to a particle of around 60 kDa as expected [22]. Addition of enough monovalent ligand **GM1 – 1** to fill all of the binding sites did not change the AUC profile. However, when sufficient divalent ligand **GM1 – 2** to fill only 10% or 20% of the binding sites was added, a second species corresponding to a dimer of LTB-pentamers started to accumulate. If the **GM1 – 2** concentration was increased to 0.5 GM1 equivalents per binding site, then the signal decreased dramatically; by this point in the titration, most of the protein had become incorporated into aggregates of sufficient size that they were rapidly sedimented to the edge of the cell, beyond the observable window in the sample cell. Curiously, if the **GM1 – 2** concentration was high enough to fill all of the LTB binding sites, then essentially all of the protein that remained in solution was in the form of dimers of pentamers. The AUC signal also decreased as the concentration of tetravalent ligand **GM1 – 4** increased (Figure 6b); however, in this case, no dimers of pentamers were observed at any ligand concentration.

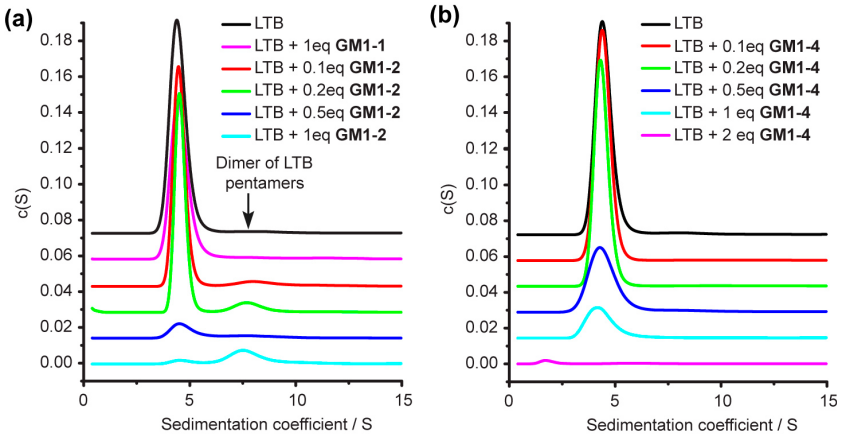

Figure 6. Sedimentation velocity analytical ultracentrifugation experiments of LTB pentamers in the presence of varying concentrations of **GM1 – 1**, **GM1 – 2** and **GM1 – 4.**

While AUC was well suited for studying the discrete species in solution, it gave little information on the formation of the larger aggregates. In contrast, dynamic light scattering (DLS) is usually dominated by the larger species present, and it can also provide more useful information on the rate of aggregation. When DLS was used to study LTB in the presence of **GM1 – 2** and **GM1 – 4** (0.1 equivalents of GM1 groups per LTB binding site), aggregates started to form within 10 minutes [22]. The **GM1 – 2** based aggregates formed more rapidly and were around 10 times larger than those derived from **GM1 – 4.** Therefore, both AUC and DLS demonstrated that the divalent and tetravalent ligands showed different solution

properties. When one considers that there is very little difference in the distances separating the oligosaccharide groups in these two ligands, the different aggregation properties must be dependent on the valencies of the two compounds.

Why does the divalent ligand give rise to dimers of pentamers, but the tetravalent ligand does not?

It was surprising that dimers of pentamers formed at low ligand:protein ratios as the ligands are sufficiently long to crosslink adjacent binding sites in the LTB pentamer. Presumably, intrapentamer binding results in rigidification of the flexible linker. If the resulting loss of conformational entropy is greater than the entropic penalty for forming a ternary complex, then the dimer of pentamers will predominate (Figure 7a). Although the tetravalent ligand could also form dimers of pentamers, in order to maximise the binding interactions they would typically involve chelating interactions, which will pay penalties for loss of conformational entropy. Alternatively, if **GM1 – 4** were to crosslink two LTB pentamers using only two of its GM1 oligosaccharides, then the other two would be preorganised to interact with other pentamers and thus lead to larger aggregates (Figure 7b). As the aggregation kinetics were slower for **GM1 – 4**, it is likely that the additional interactions in the higher valency system can overcome the conformational entropy penalty to some extent and thus the 1:1 complexes may predominate at lower ratios of ligand:protein.

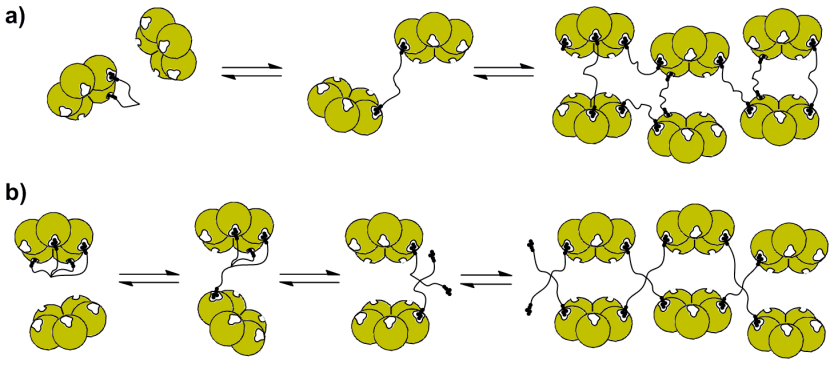

Figure 7. Dimerisation and aggregation of bacterial toxins by divalent and tetravalent ligands.

While ITC provided valuable information in the VTB-Gb3 system [16], here it only highlighted a discrepancy between the inhibitor potency in the ELISA assay and trends in binding affinity [22]. However, AUC and DLS provided complementary evidence for aggregation mechanisms and revealed for the first time that the nature of these aggregation processes can be valency-dependent.

Conclusions

Multivalent inhibitors may operate by a variety of mechanisms to enhance their potency relative to the analogous monovalent carbohydrate ligands. While individual biochemical or biophysical techniques may be sufficient to measure potency, unravelling the underlying inhibition mechanisms may require a combination of techniques. Often designs for multivalent ligands are based on static models derived from X-ray crystal structures, but dynamics of both the ligands and their multivalent protein targets can have a substantial impact on the potency of the compounds.

Acknowledgements

The author thanks The Royal Society, EPSRC, the Wellcome Trust, AstraZeneca, BBSRC and ERC COST Actions D34/0001/05 and CM1102 for financial support, and his co-authors on references [16] and [22] for assistance in preparing figures. WBT holds a Royal Society University Research Fellowship.

References

[1] Merritt, E.A., Hol, W.G.J. (1995) AB_5 toxins. *Curr. Opin. Struct. Biol.* **5:**165 – 171. doi: http://dx.doi.org/10.1016/0959-440X(95)80071-9.

[2] De Haan, L., Hirst, T.R. (2004) Cholera toxin: A paradigm for multi-functional engagement of cellular mechanisms. *Mol. Membr. Biol.* **21:**77 – 92. doi: http://dx.doi.org/10.1080/09687680410001663267.

[3] Merritt, E.A., Kuhn, P., Sarfaty, S., Erbe, J.L., Holmes, R.K., Hol, W.G.J. (1998) The 1.25 Å resolution refinement of the cholera toxin B-pentamer: Evidence of peptide backbone strain at the receptor-binding site. *J. Mol. Biol.* **282:**1043 – 1059. doi: http://dx.doi.org/10.1006/jmbi.1998.2076.

[4] Ling, H., Boodhoo, A., Hazes, B., Cummings, M.D., Armstrong, G.D., Brunton, J.L., Read, R.J. (1998) Structure of the shiga-like toxin I B-pentamer complexed with an analog of its receptor Gb_3. *Biochemistry* **37:**1777 – 1788. doi: http://dx.doi.org/10.1021/bi971806n.

[5] Turnbull, W.B., Precious, B.L., Homans, S.W. (2004) Dissecting the cholera toxin-ganglioside GM1 interaction by isothermal titration calorimetry. *J. Am. Chem. Soc.* **126:**1047 – 1054. doi: http://dx.doi.org/10.1021/ja0378207.

[6] St. Hilaire, P.M., Boyd, M.K., Toone, E.J. (1994) Interaction of the shiga-like toxin type 1 B-subunit with its carbohydrate receptor. *Biochemistry* **33:**14452 – 14463. doi: http://dx.doi.org/10.1021/bi00252a011.

[7] Mammen, M., Chio, S.-K., Whitesides, G.M. (1998) Polyvalent interactions in biological systems: Implications for design and use of multivalent ligands and inhibitors. *Angew. Chem. Int. Ed.* **37:**2755 – 2794. doi: http://dx.doi.org/10.1002/(SICI)1521-3773(19981102)37:20<2754::AID-ANIE2754>3.0.CO;2-3.

[8] Brewer, C.F., Miceli, M.C., Baum, L.G. (2002) Clusters, bundles, arrays and lattices: Novel mechanisms for lectin-saccharide-mediated cellular interactions. *Curr. Opin. Struct. Biol.* **12:**616 – 623. doi: http://dx.doi.org/10.1016/S0959-440X(02)00364-0.

[9] Lundquist, J.J., Toone, E.J. (2002) The cluster glycoside effect. *Chem. Rev.* **102:**555 – 578. doi: http://dx.doi.org/10.1021/cr000418f.

[10] Kiessling, L.L., Lamanna, A.C. (2003) Multivalency in biological systems. *NATO Science Series, II: Mathematics, Physics and Chemistry* **129:**345 – 357.

[11] Wolf, A.A., Jobling, M.G., Saslowsky, D.E., Kern, E., Drake, K.R., Kerworthy, A.K., Holmes, R.K., Lencer, W.I. (2008) Attenuated endocytosis and toxicity of a mutant cholera toxin with decreased ability to cluster ganglioside GM1 molecules. *Infect. Immun.* **76:**1476 – 1484. doi: http://dx.doi.org/10.1128/IAI.01286-07.

[12] Hayes, E.D., Turnbull, W.B. (2011) Monovalent and multivalent inhibitors of bacterial toxins. In: *Synthesis and biological applications of multivalent glycoconjugates* (Renaudet, O., Spinelli, N., Eds.), pp 78 – 91, Bentham Science Publishers. doi: http://dx.doi.org/10.2174/978160805277611101010078.

[13] Kitov, P.I., Sadowska, J.M., Mulvey, G., Armstrong, G.D., Ling, H., Pannu, N.S., Read, R.J., Bundle, D.R. (2000) Shiga-like toxins are neutralized by tailored multivalent carbohydrate ligands. *Nature* **403:**669 – 672. doi: http://dx.doi.org/10.1038/35001095.

[14] Kitova, E.N., Kitov, P.I., Bundle, D.R., Klassen, J.S. (2001) The observation of multivalent complexes of shiga-like toxin with globotriaoside and the determination of their stoichiometry by nanoelectrospray fourier-transform ion cyclotron resonance mass spectrometry. *Glycobiology* **11:**605 – 611. doi: http://dx.doi.org/10.1093/glycob/11.7.605.

[15] Kitov, P.I., Shimizu, H., Homans, S.W., Bundle, D.R. (2003) Optimization of tether length in nonglycosidically linked bivalent ligands that target sites 2 and 1 of a shiga-like toxin. *J. Am. Chem. Soc.* **125:**3284 – 3294.
doi: http://dx.doi.org/10.1021/ja0258529.

[16] Yung, A., Turnbull, W.B., Kalverda, A.P., Thompson, G.S., Homans, S.W., Kitov, P., Bundle, D.R. (2003) Large-scale millisecond intersubunit dynamics in the B subunit homopentamer of the toxin derived from escherichia coli O157. *J. Am. Chem. Soc.* **125:**13058 – 13062.
doi: http://dx.doi.org/10.1021/ja0367288.

[17] Richardson, J.M., Evans, P.D., Homans, S.W., Donohue-Rolfe, A. (1997) Solution structure of the carbohydrate-binding B-subunit homopentamer of verotoxin VT-1 from *E. coli*. *Nat. Struct. Biol.* **4:**190 – 193.
doi: http://dx.doi.org/10.1038/nsb0397-190.

[18] Stein, P.E., Boodhoo, A., Tyrrell, G.J., Brunton, J.L., Read, R.J. (1992) Crystal structure of the cell-binding B oligomer of verotoxin-1 from *E. coli*. *Nature* **355:**748 – 750.
doi: http://dx.doi.org/10.1038/355748a0.

[19] Zhang, Z., Merritt, E.A., Ahn, M., Roach, C., Hou, Z., Verlinde, C.L.M.J., Hol, W.G.J., Fan, E. (2002) Solution and crystallographic studies of branched multivalent ligands that inhibit the receptor-binding of cholera toxin. *J. Am. Chem. Soc.* **124:**12991 – 12998.
doi: http://dx.doi.org/10.1021/ja027584k.

[20] Fan, E., Zhang, Z., Minke, W.E., Hou, Z., Verlinde, C.L.M.J., Hol, W.G.J. (2000) High-affinity pentavalent ligands of *Escherichia coli* heat-labile enterotoxin by modular structure-based design. *J. Am. Chem. Soc.* **122:**2663 – 2664.
doi: http://dx.doi.org/10.1021/ja993388a.

[21] Pukin, A.V., Branderhorst, H.M., Sisu, C., Weijers, C.A.G.M., Gilbert, M., Liskamp, R.M.J., Visser, G.M., Zuilhof, H., Pieters, R.J. (2007) Strong inhibition of cholera toxin by multivalent GM1 derivatives. *ChemBioChem* **8:**1500 – 1503.
doi: http://dx.doi.org/10.1002/cbic.200700266.

[22] Sisu, C., Baron, A.J., Branderhorst, H.M., Connell, S.D., Weijers, C.A.G.M., de Vries, R., Hayes, E.D., Pukin, A.V., Gilbert, M., Pieters, R.J., Zuilhof, H., Visser, G.M., Turnbull, W.B. (2009) The influence of ligand valency on aggregation mechanisms for inhibiting bacterial toxins. *ChemBioChem* **10:**329 – 337.
doi: http://dx.doi.org/10.1002/cbic.200800550.

[23] Lebowitz, J., Lewis, M.S., Schuck, P. (2002) Modern analytical ultracentrifugation in protein science: A tutorial review. *Protein Sci.* **11:**2067 – 2079. doi: http://dx.doi.org/10.1110/ps.0207702.

[24] Schuck, P., Perugini, M.A., Gonzales, N.R., Howlett, G.J., Schubert, D. (2002) Size-distribution analysis of proteins by analytical ultracentrifugation: Strategies and application to model systems. *Biophys. J.* **82:**1096 – 1111. doi: http://dx.doi.org/10.1016/S0006-3495(02)75469-6.